

## Numerical Simulations of Intense Meiyu Rainfall in 1991 over the Changjiang and Huaihe River Valleys by a Regional Climate Model with $p$ - $\sigma$ Incorporated Coordinate System<sup>①</sup>

Liu Huaqiang (刘华强) and Qian Yongfu (钱永甫)

*Department of Atmospheric Sciences, Nanjing University, Nanjing 210093*

(Received March 30, 1998; revised June 26, 1998)

### ABSTRACT

Based on the primitive equation model with  $p$ - $\sigma$  incorporated coordinate system originally developed by Qian et al., a one-way nested fine mesh limited area model is developed. This model is nested with ECMWF T42 data to simulate the extra-intensive rainfall event occurring in the Changjiang and Huaihe River valleys in summer of 1991. The results show that the model has certain capacity to fairly reproduce the regional distribution and the movement of the main rainfall belts. Therefore it can be used as a regional climate model to simulate and predict the short-range regional climate changes.

**Key words:** Regional model, Intensive Meiyu rainfall, Numerical simulation

### 1. Introduction

Although GCMs proved successful in reproducing the basic features of large-scale atmospheric circulations (Gates, 1992), they are too coarse to describe the details of regional climate patterns (Grotch, et al., 1991). In the regions where the atmospheric dynamical and physical forcings vary on a scale of less than a few hundred kilometers, such as in the presence of complex terrain, a factor of 10 or greater increase in model horizontal resolution may be required to simulate the realistic regional responses to the future climate changes. Due to the limitations in both computational resources and representation of the relevant physical processes, the alternative approaches to regional climate modeling should be explored until the high resolution global model simulations become feasible. The basic strategy of this approach is to use the GCM to simulate the response of the general circulation to the large-scale forcings and the nested high-resolution regional climate model (RCM) to account, in a physically based way, for the local, sub-GCM-grid-scale forcings (Giorgi and Mearns, 1991). In numerical modelings, the analyzed real grid data can also be used as the boundary condition in order to remove the boundary errors produced by the large-scale models.

The numerical model with the so-called  $p$ - $\sigma$  incorporated vertical coordinate was originally developed by Qian et al., the detailed description of the redeveloped version was published in 1985 (Qian, 1985). That version was widely utilized in studying the atmospheric circulations, such as the diurnal changes of weather and climate in the Tibetan Plateau area and the development of monsoon in July (Kuo and Qian, 1981, 1982). It has

---

<sup>①</sup>Jointly Sponsored by the National Natural Science Foundation of China (No. 49735170) and the Key Project of the National Fundamental Research "Climate Dynamics and Prediction Theory".

been proven that the model has good performances both in numerical simulations and in forecasting experiments. Considering the detailed nonadiabatic physical processes contained in this model, based on it, a one-way nested fine mesh limited area model is developed and expected to be a useful RCM to simulate and predict the short-range regional climate changes.

To test the predictability of RCM, it is required to select proper weather and climate cases in which the most important physical processes, such as precipitation and temperature changes, are obvious and representative. The severe flood event happened in the summer of 1991 in the Changjiang and Huaihe River valleys is such a typical case. If a RCM can reasonably simulate or predict this severe flood event, the RCM would be considered a useful one to study the predictability of the regional climate change.

## 2. The model

### 2.1 The vertical configuration in the atmosphere

The RCM has 5 layers in the atmosphere, above the 400 hPa level the pressure coordinate is adopted and the upper atmosphere is divided into two uniform layers with a 200 hPa thickness, below the 400 hPa level the  $\sigma$  and  $\sigma_b$  coordinate systems are adopted, two  $\sigma$  layers are uniformly divided with  $\Delta\sigma = 0.5$  in the  $\sigma$  coordinate, and only one layer is defined in the special  $\sigma_b$  coordinate and taken as the atmospheric boundary layer with 50 hPa thickness everywhere. The  $\sigma$  and  $\sigma_b$  are defined as

$$\sigma = \frac{p - p_c}{p_s^*}, \quad (1)$$

$$\sigma_b = \frac{p - (p_c + p_s^*)}{\Delta p_b}, \quad (2)$$

where  $p$  is pressure,  $p_c = 400$  hPa is the thickness of the  $p$ -coordinate,  $\Delta p_b = 50$  hPa is the thickness of  $\sigma_b$ -coordinate,  $p_s^* = p_s - (p_c + \Delta p_b)$  is the thickness of the  $\sigma$ -coordinate, and  $p_s$  the surface pressure.

### 2.2 The governing equations

In the  $\sigma$ -coordinate system the dynamic equations of the atmosphere are as follows:

$$\frac{\partial u}{\partial t} = -D(u) + f_v + \nabla P_x + F_u, \quad (3)$$

$$\frac{\partial v}{\partial t} = -D(v) - fu + \nabla P_y + F_v, \quad (4)$$

$$\frac{\partial T}{\partial t} = -D(T) + \frac{R\omega T}{Pc_p} + \frac{\varepsilon}{c_p \rho} + F_T, \quad (5)$$

$$\frac{\partial q}{\partial t} = -D(q) - C + E + F_q, \quad (6)$$

$$\frac{\partial p_s}{\partial t} = -\nabla \cdot p_s^* V_4 - 2(50 \nabla \cdot V_5 - p_s^* \dot{\sigma}_{1/2}), \quad (7)$$

$$\frac{\partial \phi}{\partial \sigma} = -\frac{p_s^* RT}{(\sigma p_s^* + p_c)}, \quad (8)$$

where

$$D(A) = \vec{V} \cdot \nabla A + \sigma \frac{\partial A}{\partial \sigma},$$

$A$  represents either  $u$ ,  $v$ ,  $T$  or  $q$ .  $\nabla p$  is the horizontal pressure gradient,  $C$  is the large and cumulus condensation rates,  $E$  is the evaporation rate,  $F$  terms are the net eddy transports,  $\epsilon$  is heating rate which consists of diabatic forcings including the infrared and solar radiations. The solar radiation has both seasonal and diurnal changes. The momentum, heat and moisture fluxes in the planetary boundary layer are computed with the similarity theory (Zhang and Qian, 1999).

For simplicity, the equations for the  $p$ -coordinate can be taken as represented by the same equations by setting  $\sigma = P$ ,  $\sigma = \omega$  and  $p_s^* = 1$ . For the  $\sigma_h$  coordinate, we should set  $\sigma = \sigma_h$ ,  $\sigma = \dot{\sigma}_h$  and  $p_s^* = \Delta p_h$ .

### 2.3 The soil model and oceanic thermal model

The above 5-layer atmospheric model is coupled with a soil model and an oceanic thermal model both with two layers below the underlying surface (Qian, 1988, 1993).

### 2.4 The modeling schemes

The initial conditions and the boundary forcing are both taken from the ECMWF T42 analysis grid data set which has a horizontal resolution of  $2.5^\circ$  latitude times  $2.5^\circ$  longitude and 7 vertical levels. The lateral boundary conditions are alternated every 12 hours. A boundary condition term for the variable  $\alpha$  is given by

$$\left(\frac{\partial \alpha}{\partial t}\right)_n = w(n) \left(\frac{\partial \alpha}{\partial t}\right)_{MC} + (1 - w(n)) \left(\frac{\partial \alpha}{\partial t}\right)_{LS}, \quad (9)$$

where the subscripts LS and MC refer to the driving large-scale and the model-simulated fields, respectively. The index  $n$  refers to the number of grid points from the lateral boundaries, that is,  $n=1$  on the boundary. The values of  $w(n)$  are 0.0, 0.4, 0.7, 0.9 and 1.0 for  $n=1, 2, 3, 4$  and 5.

The model domain is from  $10^\circ\text{N}$  to  $45^\circ\text{N}$  and from  $90^\circ\text{E}$  to  $135^\circ\text{E}$ , the grid size is  $1^\circ \times 1^\circ$  in the spherical coordinate system. Ocean temperatures are obtained from monthly mean SST of 1991. We use Euler's backward method (1 hour) and the central difference method (5 hours) alternatively for time integrations with time step  $\Delta t = 3$  minutes. Initial time is set as 20:00 BST of May 1, time integration ends on 31 July. In order to compare the simulations with the observations, the simulated rainfalls are accumulated according to the observed three rainfall and two break periods.

## 3. Properties of rainfall and circulations in May to July of 1991

In May to July of 1991 a severe flood event happened in the Changjiang and Huaihe River valleys, the most severe flood took place in Jiangsu, Anhui and Hubei provinces. The monsoon rainfall (Meiyu) began on May 19 (the climatological mean datum is June 17), ended on July 16 (the climatological datum is July 10), and totally lasted for 59 days (the climatological mean length is 23 days). The total rainfall amount reached 600 to 1000 mm. There were three rainfall periods and two breaks. The first rainfall period was on May 19 to 26 with maximum precipitation on May 22 to 25, the second period was on June 2 to 17 with

maximum on June 12 to 15, and the third one was on June 30 to 16 with maximum on July 1 to 12. The two breaks with relatively less precipitation took place on May 27 to June 1 and on June 18 to 29. After July 17, the Meiyu ended and the rainfall belt moved to North China.

So far as the patterns of circulation were concerned, it was found that in that summer the ridge line of the subtropical high marched to the north of  $20^{\circ}\text{N}$  in the fourth pentad of May, almost one month earlier than usual, then it moved back and forth between  $20^{\circ}$  and  $25^{\circ}\text{N}$  during the Meiyu season. In the tropical region there was a negative SSTA area in the warm pool of the western Pacific near the Philippines, which might be responsible for the stable location of the ridge line. In high latitudes there were blocking highs over the Ural region, which made the cold air mass move southward one by one. All those patterns were favorable to the severe Meiyu in 1991.

#### 4. The simulation of movement of the western subtropical Pacific high

As it is well known, the forming, breaking and ending of Meiyu in the Changjiang and Huaihe River valleys have close relations to the advancing and withdrawing of the western Pacific subtropical high, thus, a successful simulation of rainfall in the period of Meiyu closely depends on model's performance in simulating the movement of the subtropical high. Here, we firstly display the daily averaged latitude position of 584 geopotential height (dam) line at 500 hPa along  $120^{\circ}\text{E}$  in the simulation and compare it with that in T42 data, as shown in Fig. 1. In the simulation, the time series of latitude position of 584 line is in good agreement with that in T42 data, the model can properly reproduce two obviously northward marchings of the subtropical high around the beginning and the ending of Meiyu in 1991, the model also fairly simulates the short-range northward or southward movements of the subtropical high within the period of Meiyu. However, there is a systematic error that the latitude position of 584 line in the simulation is lower than that in T42 data throughout the whole process.

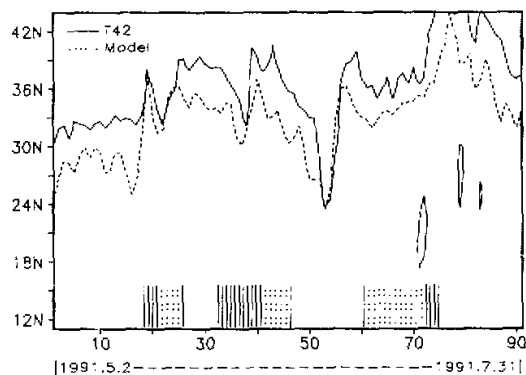


Fig. 1. The variations of daily averaged latitude positions of 584 geopotential height (dam) line at 500 hPa along  $120^{\circ}\text{E}$ . "—" and "..." over the abscissa indicate the three rainfall processes and the internal intensive rainfall sections, respectively.

## 5. Simulations of monsoon rainfall processes and breaks

To focus on the rainfall of Meiyu, we only display the simulated precipitation pattern over the area of 20–40°N, 105–125°E and compare it with observation. The verification data are taken from the daily data of 121 surface stations in this grid box.

### 5.1 Simulation of the first severe precipitation

The first severe precipitation takes place from May 19 to May 26. In this period, the averaged latitude position of the ridge line of the western Pacific high at 500 hPa is near 20°N. As shown in Fig. 2a, the observed main rainfall belt is located in the Changjiang and Huaihe River valleys with a west–east orientation, the maximum amount of rainfall is more than 200 mm. Fig. 2b shows the simulated precipitation, the simulated rainfall belt and amount are basically similar to that in Fig. 2a, however the position of the belt is somewhat southward, the area is limited to the coast, so that the observed precipitation in the upper and middle reaches of the Changjiang River is not simulated. Such discrepancy may be induced by the model spin-up process.

### 5.2 Simulation of the first break of precipitation

The first break of Meiyu happens on May 27 to June 1. In this period, the ridge line of the subtropical high moves to about 23°N, the observed main rainfall zone proceeds northward to 30–35°N, the Changjiang–Huaihe River valleys become a relatively less-precipitation area, as shown in Fig. 3a. In the simulation (see Fig. 3b), the rainfall belt is near 29°N, the rainfall amount is basically equal to observation, especially, the evident decrease of rainfall amount in the east band of that belt, the northward shift of the mid and west bands and the longitude position (near 115°E) of maximum rainfall amount center are all simulated being similar to observations. The main discrepancies in Fig. 3b are that the simulated rainbelt is too southward, the northward shift of the east band of the belt is not simulated and there is spurious precipitation between 35°N and 40°N near the north boundary.

As seen in Fig. 1, in this period, the 584 geopotential height (dam) line actually moves northward to 39°N, however, this movement in the simulation is not so evident. Consequently, the simulated rainfall belt has a lower latitude position than in reality.

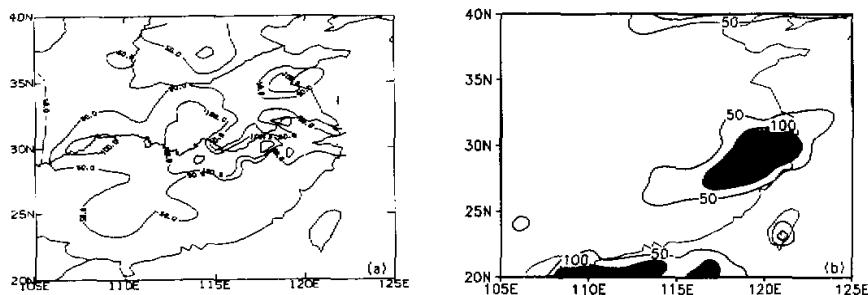


Fig. 2. Accumulated precipitation (mm) from May 15 to 26 in 1991. (a) Observed; (b) Simulated.

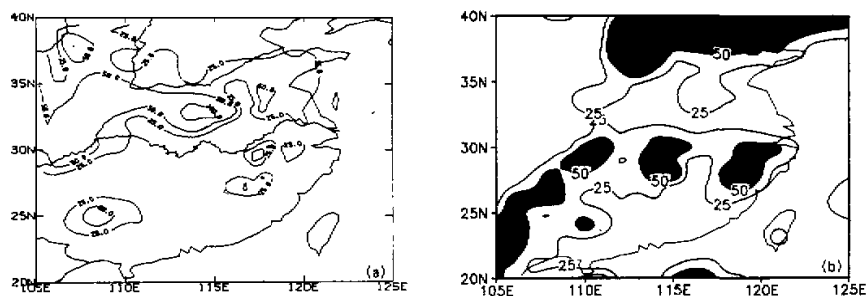


Fig. 3. The same as Fig. 2 except from May 27 to June 1.

### 5.3 Simulation of the second Meiyu rainfall

This process of precipitation takes place on June 2 to 17. In this period, as shown in Fig. 4a, the observed main rainfall belt moves back from north of  $30^{\circ}\text{N}$  to south with maximum precipitation of 300 mm and more in the middle and lower reaches of the Changjiang–Huaihe Rivers. The main rainfall belt has a west–east orientation. In the simulation (see Fig. 4b), the maximum precipitation area is well reproduced, the west–east orientation and the amount are very similar to observation. Meanwhile, the two maximum rainfall centers over Sichuan Basin and Yun–Gui Plateau are also fairly simulated. The discrepancy is that the position of the belt is a little southward.

### 5.4 Simulation of the second break

On June 18 to 29, the Meiyu is broken again due to the strengthening cold air mass from north and the withdrawal of the subtropical high ridge line to  $16^{\circ}\text{N}$ . The model has good performance in simulating such a rapid southward movement of the subtropical high (see Fig. 1). Fig. 5a shows the observed precipitation pattern. In this period, the main rainfall belt is located in the South China coast area with maximum rainfall amount of 300 mm and more, the secondary rainbelt is over the northern China with maximum precipitation of 50 mm and

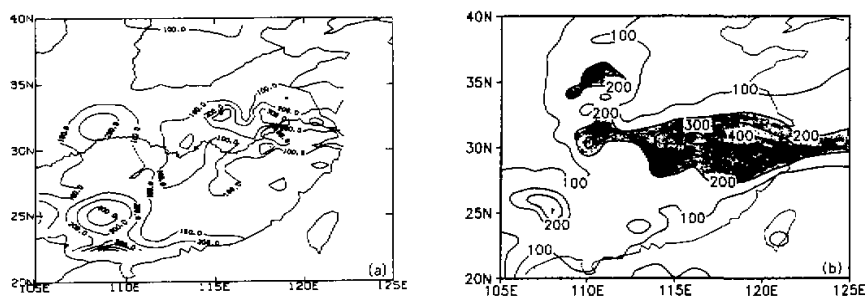


Fig. 4. The same as Fig. 2 except from June 2 to 17.

more, there is a relatively wide less-precipitation area in the Changjiang River valley and south of it. In the simulation (Fig. 5b), all above features are well simulated with a discrepancy that the relatively less-precipitation area is not so wide.

#### 5.5 Simulation of the third Meiyu process

On June 30 to July 16, the third severe precipitation takes place. In the observation (Fig. 6a), this precipitation is more severe than that in the two previous processes and concentrates to a narrow belt with the southwest-northeast orientation, in the middle and lower reaches of the Changjiang River the precipitation is specially heavy with 700 mm maximum amount in Wuhan. This precipitation process is caused by the northward movement of the ridge line of the subtropical high once again to  $23^{\circ}\text{N}$ . In the simulation (see Fig. 6b), the main rainfall zone is fairly reproduced with correct position and width, especially, there is a maximum rainfall center near Wuhan too. The discrepancy is that the amount of precipitation in the mid and east bands of rainfall belt is underestimated and will be discussed in Section 6.

#### 5.6 Simulation of the precipitation pattern after Meiyu ending

Meiyu ends on July 16 when the subtropical high ridge line moves to  $30^{\circ}\text{N}$ . The precipitation in the Changjiang-Huaihe River valleys ends too and the main rainfall zone goes to

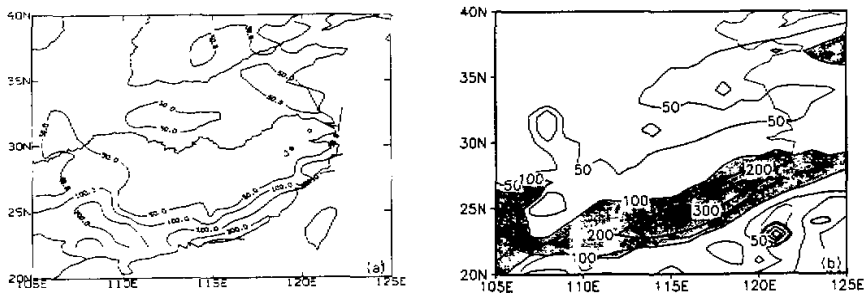


Fig. 5. The same as Fig. 2 except from June 18 to 29.

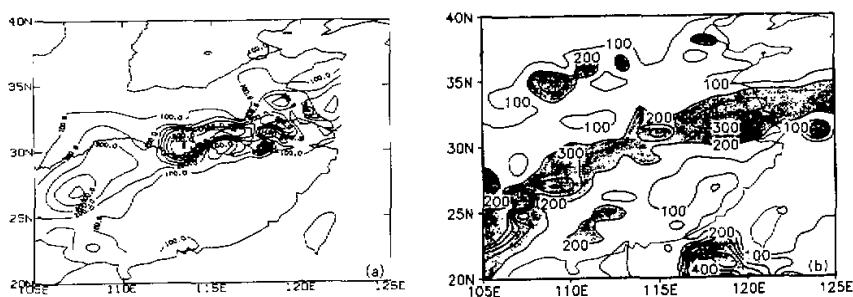


Fig. 6. The same as Fig. 2 except from June 30 to July 16.

North China. Fig. 7a shows the observed precipitation pattern on July 17 to 31, there are two main precipitation areas, one is located in the lower reaches of the Huanghe River and the other over the west part of the domain between  $105^{\circ}\text{E}$  and  $110^{\circ}\text{E}$ , a large area east of  $110^{\circ}\text{E}$  between  $25^{\circ}\text{N}$  and  $35^{\circ}\text{N}$  is a less-rainfall area with precipitation amount less than 50 mm. As seen in Fig. 7b, this pattern is simulated quite well except that the simulated two main rainfall areas are wider and the amount is larger than the observation.

It should be pointed out that the rainfall over the coast of Guangdong and Fujian Provinces is not simulated. According to the historical synoptic processes, this regional precipitation was caused by an intense tropical storm which made landfall near Shantou on July 19 with minimum center pressure less than 940 hPa. Due to the lower temporal and spatial resolutions of T42 data, the model is inadequate to simulate the structure of the tropical storm as well as the corresponding precipitation.

### 5.7 Verification on composition of simulated precipitation

To gain a better understanding of model's performance in simulating the Meiyu rainfall

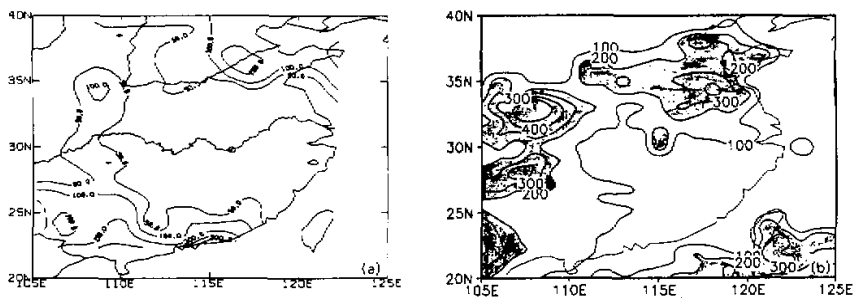


Fig. 7. The same as Fig.2 except from July 17 to 31.

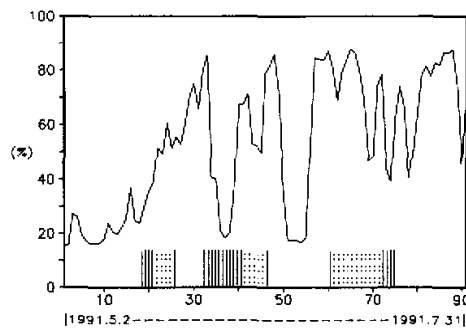


Fig. 8. The percentage of simulated convective precipitation, averaged over the area of  $27^{\circ}$ – $34^{\circ}\text{N}$ ,  $112^{\circ}$ – $122^{\circ}\text{E}$ . The abscissa is the same as that in Fig. 1.



in the summer of 1991, we do a verification on the composition of the simulated precipitation. Fig. 8 presents the percentage of the simulated convective precipitation, averaged over the area of 27–34°N, 112–122°E.

As seen in Fig. 8, the rapidly increasing of the convective rainfall is evident after the beginning of Meiyu, the intense rainfall sections (indicated by “:”) in three rainfall processes are all dominated by the convective precipitation, while the large-scale precipitation is primary in the relatively weak sections (indicated by “|”). These features of the simulated precipitation are consistent with realities of Meiyu in the summer of 1991.

## 6. Discussion and conclusions

Comparison of the simulated precipitation and observation shows that the model can fairly simulate the rainfall processes in the period of Meiyu in 1991. Meanwhile, there are some problems in the modeling, as discussed in the following.

The model's performance in the beginning stage of Meiyu (i.e. the first rainfall process and the first break) is not as good as that in the mid and later stages. This result indicates that the model spin-up time may be too long and that the model is relatively inadequate to simulate the rainfall processes in the seasonally adjusting stage of the atmospheric circulation pattern.

For the third intense rainfall process, the amount in the mid and east bands of rainfall belt is underestimated in simulation. As seen in observation (Fig. 6a), there are several meso- $\beta$  scale centers with specially heavy precipitation along the mid and east bands. The current model's resolution is not high enough to effectively simulate the meso- $\beta$  scale structure of rainbelt. This is the primary reason for underestimating the rainfall amount in simulation.

Our work leads to following conclusions:

(1) The regional climate model with  $p$ - $\sigma$  incorporated coordinate has certain capacity to simulate the severe flood event in the summer of 1991 in the Changjiang–Huaihe River valleys. Besides the positions of rainfall zones in the beginning stage of Meiyu, the area distribution and the amount of precipitation are both simulated in good agreement with observations.

(2) A better simulation of the details of rainfall distribution and amount would depend on the increase of model resolution.

(3) The lateral boundary condition is important to the regional climate modeling. In the present simulation, pseudo rainfall often takes place near the outflow boundaries and needs to be removed by further improvements of the lateral boundary condition.

## REFERENCES

- Gates, W. L., 1992: The atmospheric model intercomparison project. *Bull. Amer. Meteor. Soc.*, **73**, 1962–1970.
- Grotch, S. L., and M. C. MacCracken, 1991: The use of general circulation models to predict regional climatic change. *J. Cli.*, **4**, 286–303.
- Giorgi, F., and L. O. Mearns 1991: Approaches to the simulation of regional climate change: A review. *Rev. Geophys.*, **29**, 191–216.
- Kuo, H. L., and Qian Yongfu, 1981: Influence of the Tibetan Plateau on cumulative and diurnal changes of weather and climate in summer. *Mon. Wea. Rev.*, **109**, 2337–2356.
- Kuo, H. L., and Qian Yongfu, 1982: Numerical simulation of the development of mean monsoon circulation in July. *Mon. Wea. Rev.*, **110**, 1879–1897.

- Qian Yongfu, 1985: A five-layer primitive equation model with topography. *Plateau Meteorology*, **4**(2), 1–28 (in Chinese).
- Qian Yongfu, 1988: A scheme of calculation of heat balance temperature at ground surface. *Meteorologica Sinica*, **4**, 14–27 (in Chinese).
- Qian Yongfu, 1993: The effects of different sea surface temperature distributions over the western Pacific on the summer monsoon properties. *Acta Oceanologica Sinica*, **12**(4), 535–547.
- Zhang Qiong, and Qian Yongfu, 1999: Effects of boundary layer parameterization on the monthly mean simulation. *Acta Meteorologica Sinica*, **13**, 73–85.
-